Low-energy ηN interactions: scattering lengths and resonance parameters

R. A. Arndt, W. J. Briscoe, T. W. Morrison, I. I. Strakovsky, and R. L. Workman
Center for Nuclear Studies, Physics Department
The George Washington University, Washington, D.C. 20052

A. B. Gridnev
Petersburg Nuclear Physics Institute, Gatchina
St. Petersburg 188350, Russia

(Dated: February 9, 2008)

We consider the impact of two recent $\pi^- p \to \eta n$ measurements on the ηN scattering length and ηN branching fractions for the $N(1535)$ and $N(1520)$ resonances within a coupled-channel analysis of πN elastic scattering and ηN production data. The sensitivity of these results to model input is also explored.

PACS numbers: 13.75.-n, 25.80.-e, 13.30.Eg, 11.80.Et

I. INTRODUCTION

While most of our knowledge of the N and Δ baryons has come from πN elastic scattering and photoproduction, the ηN channel has been crucial in determinations of the $N(1535)$ properties. In πN elastic scattering, this resonance signal is masked by a sharp cusp due to the opening ηN channel, while in the reactions $\pi^- p \to \eta n$ and $\gamma p \to \eta p$, the $N(1535)$ is associated with a rapidly increasing cross section near threshold. As a result, the incorporation of eta-production data in multi-channel fits has allowed more reliable determinations of the $N(1535)$ resonance parameters.

The nearby $N(1520)$ resonance, while not strongly coupled to the ηN channel, gives an important contribution to some eta-production observables through interference effects. The Particle Data Group [1] estimates the ratio $\Gamma_{\eta N}/\Gamma_{\rm tot}$ to be 0.0023 ± 0.0004, a value determined mainly by the multi-channel analysis of Penner and Mosel [2]. In $\pi^- p \to \eta n$, the effect of this resonance is visible in the departure from purely S-wave behavior with increasing energy. While the $N(1520)$ contribution is small, the effect is magnified through S-D wave interference with the dominant $N(1535)$ contribution. In ηN photoproduction, this interference effect is particularly evident in measurements with a polarized beam (Σ) [3].

The ηN interaction has also been studied extensively due to a strong attraction at low energies, observed in most analyses, which could possibly lead to the existence of bound state η-mesic nuclei [4, 5]. Unfortunately, the ηN scattering length cannot be measured directly. Instead, cross sections for η meson production, $\pi^- p \to \eta n$ and $\gamma p \to \eta p$, have been studied [6, 7, 8, 9, 10, 11, 12, 13, 14, 15, 16, 17, 18, 19, 20]. In Ref. [21], it was demonstrated that the real part of the scattering length cannot be extracted directly from the low-energy eta-production cross sections and a model analysis is needed. Previous analyses [2, 5, 8, 21, 22, 23, 24, 25, 26, 27, 28, 29, 30, 31, 32, 33, 34, 35, 36, 37, 38, 39, 40, 41, 42, 43, 44, 45, 46, 47, 48, 49, 50] have found a large spread for the real part, from a negative value [21] to 1 fm [50] (Table I). Reasons for the spread include the rather old and conflicting η meson production data and differing πN elastic scattering amplitudes from the Karlsruhe [51] and SAID [52] groups. However, the largest factor appears to be the model used in analyzing the data.

In recent years, the eta-production database has seen significant improvements. In this paper, we present the results from analyses of these new data. The most recent data for the reaction $\pi^- p \to \eta n$ are described in Section II. In Section III, we described the formalism associated with our fits. Results and comparisons with previous determinations are tabulated in Section IV. Finally, in Section V, we summarize our findings and consider the open questions which will require further work.

II. THE EXPERIMENTAL DATABASE

Until recently, the $\pi^- p \to \eta n$ cross section database contained mainly old and often conflicting measurements (see Ref. [53] for details), with no polarized measurements existing below 1.1 GeV/c [54]. These older data have been reviewed by Clajus and Nefkens [55]. More recently, differential and total cross sections for $\pi^- p \to \eta n$ near threshold have been measured using the BNL-AGS Facility (E909) [6]. Data were obtained from threshold ($p_\pi = 684.5$ MeV/c) to ∼770 MeV/c.

The most recent $\pi^- p \to \eta n$ experiment was also performed at BNL, but in this case, using the Crystal Ball spectrometer (now moved to MAMI at Mainz). Cross sections were measured from threshold to 747 MeV/c (E913/914) [7]. The total and differential cross sections from these two BNL measurements are compared in Fig. 1. Normalization issues still remain for the differential cross sections. However, the Crystal Ball distributions show a much smoother variation and a clear onset of higher partial-wave contributions with increasing energy. This feature, which is a vast improvement over previous measurements, allows an improved separation of the $N(1520)$ contribution.

Traditionally, the total cross-section is plotted as a function of the pion laboratory energy [Fig 1(h)]. This view shows the sharp growth above threshold which is usually attributed to the dominance of the $N(1535)$ resonance, having a mass close to the η production threshold ($\sqrt{s} =$ 1487 MeV) and a strong coupling to the ηN system. In Fig. 2, we instead plot the total cross-section as a function of the η cm momentum p^*_η. From the figure, we see that data can be described very well by a linear fit (dashed line). This is due to the S-wave dominance of the total cross section. From the slope of the best-fit line, a restriction on the imaginary part of the ηN elastic scattering amplitude $A_{\eta N}$ can be found.

The optical theorem leads to

$$\begin{aligned} ImA_{\eta N} &= \frac{p^*_\eta}{4\pi}\ \sigma^{tot}_{\eta n} \\ &= \frac{p^*_\eta}{4\pi}\ (\sigma_{\eta n\to\pi N} + \sigma_{\eta n\to 2\pi N} + \sigma_{\eta n\to\eta n}) \\ &= \frac{3\ p^{*2}_\pi}{8\pi p^*_\eta}\ \sigma_{\pi^- p\to\eta n} + \frac{p^*_\eta}{4\pi}\ (\sigma_{\eta n\to 2\pi N} + \sigma_{\eta n\to\eta n}). \end{aligned} \tag{1}$$

As a result, we have

$$ImA_{\eta N} \geq \frac{3p^{*\,2}_\pi}{8\pi p^*_\eta}\ \sigma_{\pi^- p\to\eta n}. \tag{2}$$

Using a linear fit, the recent E909 threshold data [6] give

$$\begin{aligned} &\frac{1}{p^*_\eta}\sigma_{\pi^- p\to\eta n} = 15.2 \pm 0.8\ \mu\text{b/MeV} \\ &ImA_{\eta N} \geq 0.172 \pm 0.009\ \text{fm}, \end{aligned} \tag{3}$$

which can be compared with a previous output from Ref. [8]

$$\begin{aligned} &\frac{1}{p^*_\eta}\sigma_{\pi^- p\to\eta n} = 21.2 \pm 1.8\ \mu\text{b/MeV and} \\ &ImA_{\eta N} \geq 0.24 \pm 0.02\ \text{fm}. \end{aligned} \tag{4}$$

It is commonly believed that the $N(1535)$ resonance dominates the η production cross section. This resonance mechanism results in the imaginary part of the η pion-production and the ηN elastic scattering amplitudes being determined mainly by the $N(1535)$ resonance parameters. But this is not the case for the real part. The real part of the resonance amplitude goes to zero at the resonance position. Therefore, the real part of the ηN scattering length strongly depends on nonresonant processes. For this reason, a multichannel analysis is favored in determining the ηN scattering length. Our approach is described in the next section.

III. COMBINED ANALYSIS OF πN ELASTIC AND $\pi^- p \to \eta n$ DATA

Our energy-dependent partial-wave fits are parametrized in terms of a coupled-channel Chew-Mandelstam K matrix, as described in Ref. [53]. This choice determines the way we modify energy dependence and account for unitarity in our fits. Data for πN elastic scattering have been fitted up to 2.1 GeV in the pion lab kinetic energy. Data for the reaction $\pi^- p \to \eta n$ have been included from threshold up to 0.8 GeV. Constraint data have also been included, in order to ensure that the resulting fit produces elastic πN amplitudes satisfying a set of forward and fixed-t dispersion-relations. This fit to data plus constraints must be iterated until a stable result is obtained [53]. Finally, we have included $\pi\Delta$ and ρN channels to account for unitarity, but have not explicitly fitted data of this type.

The $N(1535)$ resonance couples mainly to πN and ηN, with a much smaller branching fraction to $\pi\pi N$, and our results were not sensitive to the choice of additional channels. For the $N(1520)$, however, there is a substantial inelastic branching to $\pi\pi N$, split mainly between ρN and $\pi\Delta$. We therefore considered two different fits having (a) approximately equal ρN and $\pi\Delta$ branching fractions, and (b) a larger ρN branching fraction. While this choice had little effect on the total width, it significantly changed the branching to ηN.

In order to extract resonance parameters from our global fits, we have generally extrapolated into the complex energy plane to search for poles. We have also fitted our energy-dependent and single-energy partial-wave amplitudes with Breit-Wigner plus background forms. Here we have chosen to fit the partial waves containing the $N(1535)$ and $N(1520)$ resonances in terms of a K-matrix resonance form, allowing for 2 poles in the S_{11} partial wave, plus background. This revised parametrization was then fitted directly to the data (from 400 to 900 MeV in the pion kinetic energy) in order to determine resonance parameters. The remaining partial waves were fixed to values determined from a previous global (energy-dependent) fit. This resulted in error estimates more directly tied to the data.

The general form used for the modified (S_{11} and D_{13}) partial waves was

$$T \;=\; \rho^{1/2}\, T_x\, \rho^{1/2}, \tag{5}$$

with ρ^i giving the phase space for a channel (πN, $\pi\Delta$, ρN, or ηN), and with T_x represented in terms of a K-matrix as

$$T_x \;=\; K_x \left(1 + iK_x\right)^{-1}, \tag{6}$$

where, in a two-resonance case, we have fitted

$$K_x \;=\; K_b \;+\; \frac{K_1}{W_1 - W} \;+\; \frac{K_2}{W_2 - W}. \tag{7}$$

The background has been parametrized in terms of the phase space, $K_b^{ij} = (\rho^i \rho^j)^{1/2} \kappa^{ij}$, with κ^{ij} elements assumed constant over the limited energy ranges of these fits. The K-matrix pole residues were similarly parametrized as $K_1^{ij} = \gamma^i \gamma^j$ with $\gamma^i = (\rho^i \Gamma^i/2)^{1/2}$. The phase phase factors were normalized to unity at the resonance position (W_1).

Results for the S_{11} and D_{13} πN elastic scattering amplitudes are displayed in Fig. 3. Here the result of our most recently published fit (FA02) is compared to an updated and improved version (G380). The K-matrix fits closely follow the G380 result and have not been plotted. Fig. 4 shows the much larger deviations existing between different versions of the $\pi^- p \to \eta n$ amplitudes.

IV. RESULTS AND DISCUSSION

A. ηN couplings

Our results from four fits, two with and two without the recent Crystal Ball data, are summarized in Tables II,III. Listed are the partial widths for the $N(1535)$ and $N(1520)$ resonances. While the PDG quotes [1] a broad and conservative range of about 30 to 50 percent for both the πN and

ηN branching ratios corresponding to the $N(1535)$, most recent determinations have found the ηN fraction to be about 50%, the remaining 50% divided between the πN and $\pi\pi N$ channels. We have similarly found ηN branching fractions exceeding the πN fraction in all of our fits. The $N(1535)$ total width, found in the K-matrix fits, differs significantly from our previously published result [53]. This is due to the coupled-channel K-matrix form more than a qualitative difference in the partial-wave amplitudes. We note that coupled-channel fits have in the past [56] found the N(1535) width to be about half the 200 MeV obtained in single-channel fits to eta photoproduction [57].

The extracted $N(1520)$ ηN branching fraction is very small, as was expected. Penner and Mosel [2] found 0.0023±0.0004 for this ratio using an older version of our πN amplitudes as a representation of the πN elastic scattering database. A somewhat smaller value, 0.0008±0.0001 was found in a Mainz analysis of eta photoproduction data [3]. We find this quantity to be rather sensitive to model details, but our range of values effectively spans the two previous determinations. Fits A and C have included the Crystal Ball data, and result in more precisely determined ηN branching fractions, as expected. In fits B and D, the Crystal Ball data were excluded. Different ρN and $\pi\Delta$ branching fractions (Fits A and B versus C and D) were obtained through the choice of contributions to the background. The background K-matrix contains elements coupling, for example, $\eta N \to \rho N$, which cannot be measured and are therefore intrinsically model-dependent.

B. ηN scattering length

As can be seen in Table I, previous determinations of the ηN scattering length have produced widely varying results. This should not be surprising, as these determinations require the threshold behavior of an amplitude that cannot be directly measured. Somewhat surprising to us, however, was the relative stability of scattering lengths found from our set of four K-matrix fits, with and without the Crystal Ball data, which are shown in Table IV. These results are comparable to those found in a fit by Green and Wycech [48], who used a similar K-matrix representation for the S-wave amplitudes, and the multi-channel fits of Penner and Mosel [2]. If, however, we determine the ηN scattering length directly from our global fit, based on a Chew-Mandlestam K-matrix formalism, a very different result is found. This value seems more compatible with the calculation of Ref. [36]. As a result, we can confirm previous determinations within similar approaches, but caution that (for the real part in particular) the employed model may be more important than improvements in the fitted data. The S-wave ηn elastic partial waves, from G380 and Fit A, are displayed in Fig. 5.

V. CONCLUSIONS AND FUTURE PROSPECTS

We have explored the model and data dependence of ηN couplings to the $N(1535)$ and $N(1520)$ resonances, and have extracted the ηN scattering length. Our values for these quantities are in reasonable agreement with previous determinations. One notable difference in our method has been the direct fit to data, rather than to amplitudes. This has allowed a direct χ^2 comparison of the fits.

From an experimental point of view, several issues remain to be resolved. The recent Crystal Ball measurements of $\pi^- p \to \eta n$, covering a region from threshold to the peak of the $N(1535)$ resonance, have suggested a slightly lower mass and width for this state. This could have been verified with measurements continuing to higher energies. However, with the Crystal Ball moved to Mainz, this is no longer possible. The standard value [1] (547.75±0.12 MeV) of the η mass has also shifted recently, and this naturally effects extrapolations associated with the scattering length determination. The linear plot in Fig. 2 has taken 547.3 MeV for the eta meson mass. We have allowed the eta mass to vary between 547 and 548 MeV, finding very little sensitivity in our fits. We should also note that a recent measurement from the GEM collaboration [58] finds a value close to the previous "standard" mass of 547.3 MeV.

Given the model dependence found in our determinations, it would be interesting to see the effect of the Crystal Ball data in multi-channel fits which include representations of the $\pi N \to \pi\pi N$ data. Also of interest would be a re-examination of the $N(1520)$ ηn branching fraction as extracted from eta-photoproduction data. The quality and quantity of data for this reaction has increased since the Mainz analysis [3]. Work on this subject is in progress.

Acknowledgments

This work was supported in part by the U. S. Department of Energy under Grants DE–FG02–95ER40901 and DE–FG02–99ER41110. R. A, I. S., and R. W. acknowledge partial support from Jefferson Lab, which is operated by the Southeastern Universities Research Association under DOE contract DE–AC05–84ER40150. A. G. acknowledges the hospitality extended by the Center for Nuclear Studies of The George Washington University.

---

[1] S. Eidelman *et al.* [Particle Data Group], Phys. Lett. B **592**, 1 (2004).
[2] G. Penner and U. Mosel, Phys. Rev. C **66**, 055211, (2002) [nucl-th/0207066].
[3] L. Tiator, D. Drechsel, G. Knöchlein, and C. Bennhold, Phys. Rev. C **60**, 035210 (1999) [nucl-th/9902028].
[4] G. A. Sokol, A. I. L'vov, and L. N. Pavlyuchenko, *Proceedings of the Workshop on the Physics of Excited Nucleons (NSTAR2001), Mainz, Germany, March, 2001*, edited by D. Drechsel and L. Tiator (World Scientific, 2001) p. 283 [nucl-ex/0106005].
[5] R. S. Bhalerao and L. C. Liu, Phys. Rev. Lett. **54**, 865 (1985);
Q. Haider and L. C. Liu, Phys. Lett. B **172**, 257 (1986).
[6] T. W. Morrison *et al.*, Bull. Am. Phys. Soc. **45**, 58 (2000),
T. W. Morrison, Ph. D. Thesis, The George Washington University, Dec. 1999.
[7] S. Prakhov *et al.* [Crystal Ball Collaboration], in press, Phys. Rev. C **72**, (2005).
[8] D. M. Binnie *et al.*, Phys. Rev. D **8**, 2789 (1973).
[9] F. Bulos *et al.*, Phys. Rev. **187**, 1827 (1969).
[10] N. C. Debenham *et al.*, Phys. Rev. D **12**, 2545 (1975).
[11] W. Deinet *et al.*, Nucl. Phys. **B11**, 495 (1969).
[12] B. W. Richards *et al.*, Phys. Rev. D **1**, 10 (1970).
[13] B. Krushe *et al.*, Phys. Rev. Lett. **74**, 3736 (1995).
[14] J. W. Price *et al.*, Phys. Rev. C **51**, 2283 (1995).
[15] F. Renard *et al.* [GRAAL Collaboration], Phys. Lett. B **528**, 215 (2002) [hep-ex/0011098].
[16] B. Delcourt *et al.*, Phys. Lett. B **29**, 75 (1969).
[17] S. A. Dytman *et al.*, Phys. Rev. C **51**, 2710 (1995).
[18] R. Erbe *et al.* (Aachen-Berlin-Bonn-Hamburg-Heidelberg-München Collaboration), Phys. Rev. **175**, 1669 (1968).
[19] M. Dugger *et al.* [CLAS Collaboration], Phys. Rev. Lett. **89**, 222002 (2002).
[20] V. Crede *et al.* [CB–ELSA Collaboration], Phys. Rev. Lett. **94**, 012004 (2005) [hep-ex/0311045].
[21] B. L. Birbrair and A. B. Gridnev, Z. Phys. A **354**, 95 (1996).
[22] N. Kaiser T. Waas, and W. Weise, Nucl. Phys. **A612**, 297 (1997) [hep-ph/9607459].
[23] C. Bennhold and H. Tanabe, Nucl. Phys. **A530**, 625 (1991).
[24] B. Krusche, in *Proc. of the II TAPS Workshop, Guadamar, Spain, 1993*, edited by J. Diaz and Y. Schutz (World Scientific, 1994), p. 310.
[25] V. Yu. Grishina *et al.*, Phys. Lett. B **475**, 9 (2000) [nucl-th/990549].
[26] J. Caro Ramon *et al.*, Nucl. Phys. **A672**, 249 (2000) [nucl-th/9912053].
[27] M. Batinic *et al.*, Phys. Rev. C **52**, 2188 (1995) [nucl-th/9502017].
[28] A. Sibirtsev *et al.*, Phys. Rev. C **65**, 044007 (2002) [nucl-th/0111086].
[29] O. Krehl *et al.*, Phys. Rev. C **62**, 025207 (2000) [nucl-th/9911080].
[30] W. Briscoe *et al.*, *Proceedings of the 9th International Symposium on Meson-Nucleon Physics and the Structure of the Nucleon (MENU2001), Washington, DC, USA, July, 2001*, edited by H. Haberzettl and W. J. Briscoe, πNNewslett, **16**, 391 (2002).
[31] G. Fäldt and C. Wilkin, Nucl. Phys. **A587**, 769 (1995).
[32] L. Tiator *et al.*, Nucl. Phys. **A580**, 455 (1994) [nucl-th/9404013].
[33] T. Feuster and U. Mosel, Phys. Rev. C **58**, 457 (1998) [nucl-th/9708051].
[34] Ch. Sauermann, B. L. Frieman, and W. Nörenberg, Phys. Lett. B **341**, 261 (1995) [nucl-th/9408012];
Ch. Deutsch-Sauermann, B. L. Frieman, and W. Nörenberg, Phys. Lett. B **409**, 51 (1997) [nucl-th/9701022].
[35] N. Willis *et al.*, Phys. Lett. B **406**, 14 (1997) [nucl-ex/9703002].
[36] B. Krippa, Phys. Rev. C **64**, 047602 (2001).
[37] C. Wilkin, Phys. Rev. C **47**, R938 (1993) [nucl-th/9301006].
[38] V. V. Abaev and B. M. K. Nefkens, Phys. Rev. C **53**, 375 (1996).

[39] N. Kaiser, P. B. Siegel, and W. Weise, Phys. Lett. B **362**, 23 (1995) [nucl-th/9507036];
N. Kaiser *et al.*, Nucl. Phys. **A594**, 325 (1995) [nucl-th/9505043].
[40] M. Batinic *et al.*, nucl-th/9703023.
[41] M. Batinic *et al.*, Phys. Scr. **58**, 15 (1998).
[42] A. M. Green and S. Wycech, Phys. Rev. C **55**, R2167 (1997) [nucl-th/9703009].
[43] S. A. Rakityansky *et al.*, Nucl. Phys. **A684**, 383 (2001);
N. V. Shevchenko *et al.*, Phys. Rev. C **58**, 3055 (1999) [nucl-th/9808009].
[44] A. Fix and H. Arenhövel, Phys. Rev. C **66**, 024002 (2002).
[45] J. Nieves and E. Ruiz Arriola, Phys. Rev. D **64**, 116008 (2001) [hep-ph/0104307].
[46] S. F. Tuan, Phys. Rev. **139B**, 1393 (1965).
[47] A. M. Green and S. Wycech, Phys. Rev. C **60**, 035208 (1999) [nucl-th/9905011].
[48] A. M. Green and S. Wycech, Phys. Rev. C **71**, 014001 (2005) [nucl-th/0411024].
[49] M. Batinic *et al.*, Phys. Rev. C **51**, 2310 (1995) [nucl-th/9501011].
[50] M. Arima *et al.*, Nucl. Phys. **A543**, 613 (1992).
[51] G. Höhler, *Pion–Nucleon Scattering*, Landoldt–Börnstein Vol. **I/9b2**, edited by H. Schopper (Springer Verlag, 1983).
[52] R. A. Arndt, R. L. Workman, I. I. Strakovsky, and M. M. Pavan, Phys. Rev. C **52**, 2120 (1995) [nucl-th/9505040].
[53] R. A. Arndt, W. J. Briscoe, I. I. Strakovsky, R. L. Workman, and M. M. Pavan, Phys. Rev. C **69**, 035213 (2004) [nucl-th/0311089].
[54] The full database and numerous PWAs can be accessed at the website http://gwdac.phys.gwu.edu.
[55] M. Clajus and B. M. K. Nefkens, πN Newslett. **7**, 76 (1992).
[56] T. P. Vrana, S. A. Dytman, and T. S. H. Lee, Phys. Rept. **328**, 181 (2000) [nucl-th/9910012].
[57] B. Krusche, N. C. Mukhopadhyay, J. F. Zhang, and M. Benmerrouche, Phys. Lett. B **397**, 171 (1997).
[58] M. Abdel-Bary *et al.* [GEM Collaboration], "A precision determination of the mass of the η meson", [hep-ex/0505006].

TABLE I: ηN-scattering length overview

$A_{\eta N}$ (fm)	Reference	$A_{\eta N}$ (fm)	Reference
-0.15 +i 0.22	[21]	0.56 +i 0.22	[21]
0.20 +i 0.26	[22]	0.577 +i 0.216	[33]
$\geq$i 0.24(2)	[8]	0.579 +i 0.399	[24]
0.25 +i 0.16	[23]	0.621(40) +i 0.306(34)	[38]
0.27 +i 0.22	[5]	0.68 +i 0.24	[39]
0.28 +i 0.19	[5]	0.717(30) +i 0.263(25)	[40]
0.281 +i 0.360	[24]	0.734(26) +i 0.269(19)	[41]
$\leq$0.30	[25]	0.75(4) +i 0.27(3)	[42]
0.32 +i 0.25	[26]	$\geq$0.75	[43]
0.404(117)+i 0.343(58)	[27]	0.75 +i 0.27	[44]
0.42 +i 0.34	[28]	0.772(5) +i 0.217(3)	[45]
0.42 +i 0.32	[29]	0.83 +i 0.35	[46]
0.430 +i 0.394	[24]	0.87 +i 0.27	[47]
0.46(9) +i 0.18(3)	[30]	0.876(47) +i 0.274(39)	[27]
0.476 +i 0.279	[31]	0.886(47) +i 0.274(39)	[27]
0.476 +i 0.279	[32]	0.91(6) +i 0.27(2)	[48]
0.487 +i 0.171	[33]	0.91(3) +i 0.29(4)	[49]
0.51 +i 0.21	[34]	0.968 +i 0.281	[27]
0.52 +i 0.25	[35]	0.980 +i 0.37	[50]
0.54 +i 0.49	[36]	0.991 +i 0.347	[2]
0.55(20) +i 0.30	[37]	1.05 +i 0.27	[47]
0.550 +i 0.300	[34]		

TABLE II: The present (G380) and previous (FA02 [53] energy-dependent partial-wave analyses of elastic $\pi^{\pm}p$, charge-exchange ($\pi^0 n$), and $\pi^- p \to \eta n$ (ηn) scattering data, compared to fits A - D from 400 – 900 MeV.

Solution	$\chi^2/\pi^- p$	$\chi^2/\pi^0 n$	$\chi^2/\eta n$
FA02	6286/2773	1920/1100	635/257
G380	5825/2773	1723/1100	569/257
Fit A	5961/2773	1684/1100	539/257
Fit B	5935/2773	1748/1100	575/257
Fit C	6001/2773	1732/1100	571/257
Fit D	5961/2773	1839/1100	582/257

TABLE III: Resonance widths (in MeV) and branching fractions.

Resonance	Solution	Γ_π	Γ_η	$\Gamma_{\pi\Delta}$	$\Gamma_{\rho N}$	$\Gamma_\eta/\Gamma_{\rm tot}$
N(1535)	Fit A	30±2	45±3	15±1		0.50
	Fit B	32±3	45±4	16±1		0.48
	Fit C	39±3	67±4	9±2		0.58
	Fit D	42±6	70±10	11±2		0.57
N(1520)	Fit A	68±1	0.12±0.03	19±5	19±5	0.0012
	Fit B	68±1	0.17±0.12	19±6	19±6	0.0016
	Fit C	67±1	0.08±0.03	14±4	24±4	0.0008
	Fit D	67±1	0.09±0.07	14±5	24±5	0.0009

TABLE IV: ηN scattering lengths from K-matrix fits (resonance plus background, see text) and the global energy-dependent fit (G380).

Solution	Scattering Length (fm)
Fit A	1.14 + i 0.31
Fit B	1.10 + i 0.30
Fit C	1.12 + i 0.39
Fit D	1.03 + i 0.41
G380	0.41 + i 0.56

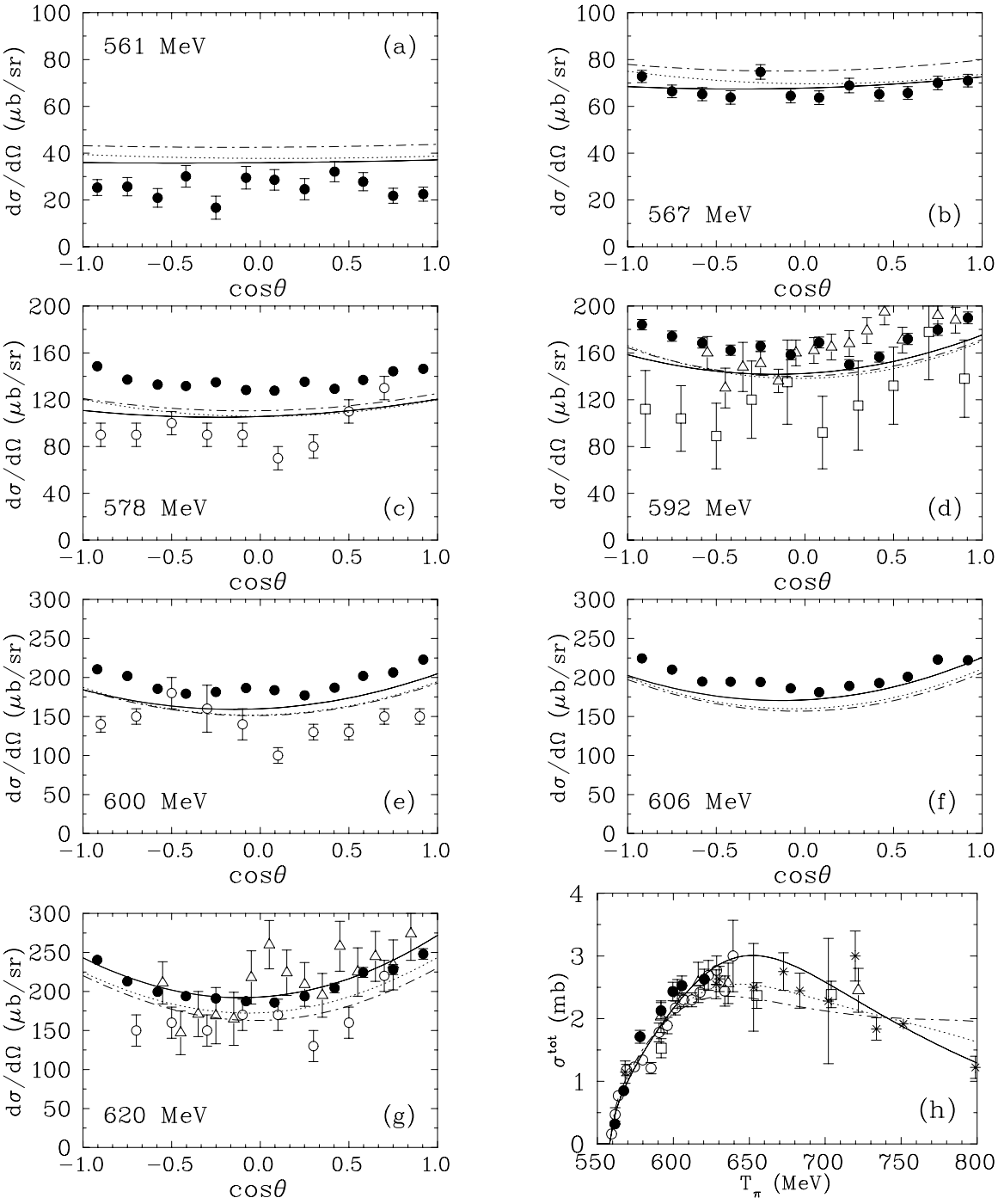

FIG. 1: (a)–(g) Differential cross sections for $\pi^- p \to \eta n$ at seven incident π^- energies. The uncertainties are statistical only. For the total cross sections (h), we have combined statistical and systematic uncertainties in quadrature. FA02 [53] (E913/E914 data not included), G380, and Fit A shown as solid, dash-dotted, and dotted lines, respectively. Experimental data are from [7] (filled circles), [6] (open circles), [11] (open triangles), and [12] (open squares) measurements. Other previous measurements (for references see SAID database [54]) shown as asterisks.

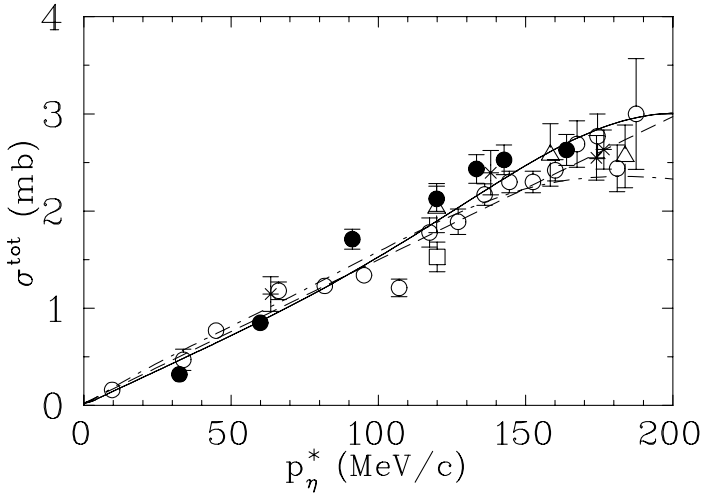

FIG. 2: p^*_η dependence of $\sigma^{tot}(\pi^- p \to \eta n)$. Data and notation given in Fig. 1. Dashed line shows a linear fit to E909 [6] (open circles) data.

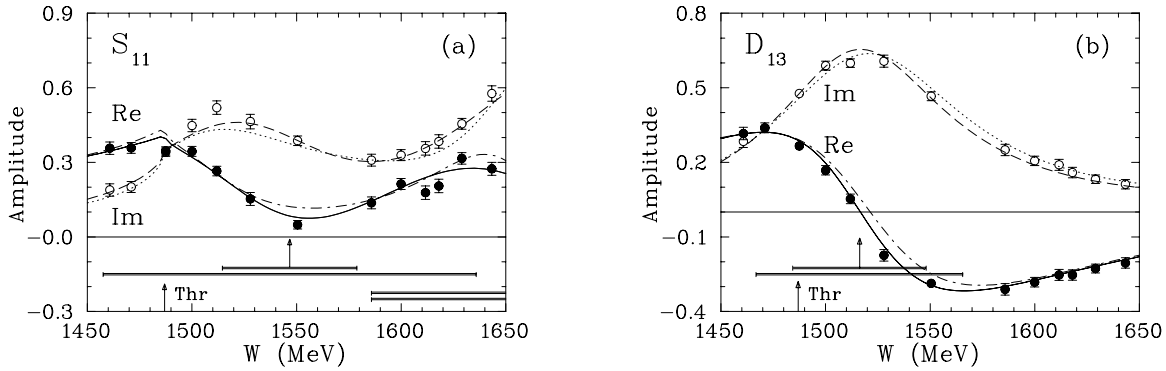

FIG. 3: (a) S_{11} and (b) D_{13} partial amplitudes for πN elastic scattering. Solid (dashed) curves give the real (imaginary) parts of amplitudes corresponding to the predictions of solution FA02 [53] (E913/E914 data not included). Single-energy solutions associated with FA02 are plotted as filled and open circles. Dash-dotted (dotted) curves show the real (imaginary) parts of amplitudes corresponding to G380. Differences between G380 and Fit A are not significant. All amplitudes are dimensionless. Vertical arrows indicate W_R and horizontal bars show full $\Gamma/2$ and partial widths for $\Gamma_{\pi N}$ associated with the FA02 results.

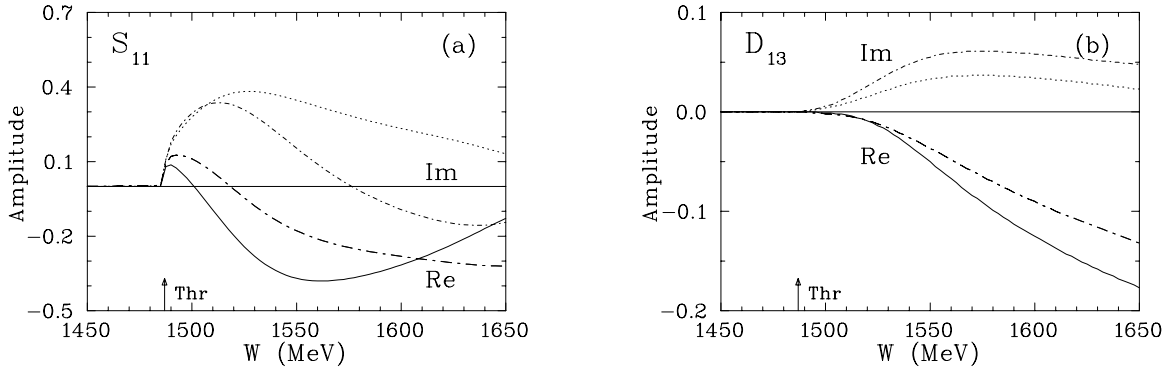

FIG. 4: (a) S_{11} and (b) D_{13} partial amplitude for $\pi^- p \to \eta n$. Dash-dotted (dotted) curves show the real (imaginary) parts of amplitudes corresponding to G380. Solid (short-dash-dotted) lines represent the real (imaginary) parts of amplitudes corresponding to the Fit A. All amplitudes are dimensionless.

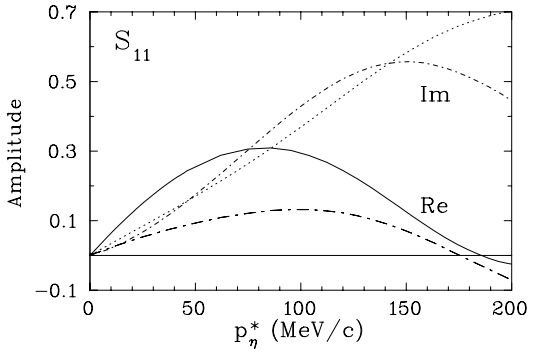

FIG. 5: p^*_η dependence of the S_{11} amplitude for the reaction $\eta n \to \eta n$. Dash-dotted (dotted) curves give the real (imaginary) parts of amplitudes corresponding to the solution G380. Solid (short-dash-dotted) lines represent the real (imaginary) parts of amplitudes Fit A. All amplitudes are dimensionless.